



Contents lists available at ScienceDirect

Tetrahedron

journal homepage: www.elsevier.com/locate/tet

Modulation of imine chemistry with intramolecular hydrogen bonding: Effects from *ortho*-OH to NH

Zelin Feng^{a, b, 1}, Shuaipeng Jia^{a, b, 1}, Hang Chen^{b, c, **}, Lei You^{b, c, *}

^a College of Chemistry, Fuzhou University, Fuzhou 350116, PR China

^b State Key Laboratory of Structural Chemistry, Fujian Institute of Research on the Structure of Matter, Chinese Academy of Sciences, Fuzhou 350002, PR China

^c University of Chinese Academy of Sciences, Beijing 100049, PR China

ARTICLE INFO

Article history:

Received 14 January 2020

Received in revised form

1 March 2020

Accepted 13 March 2020

Available online xxx

Keywords:

Imine bond

Hydrogen bond

Dynamic covalent chemistry

Component exchange

Salicylaldehyde

ABSTRACT

Salicylaldehyde derivatives and their imines are important building blocks in organic and supramolecular chemistry. In an effort to expand structural diversity in the current work we changed *ortho*-OH in salicylaldehyde to NH of amide/sulfonamide and investigated the effect of resulting intramolecular hydrogen bonds on imine dynamic covalent chemistry (DCC). A suite of *ortho*-aminobenzaldehydes were readily synthesized, and X-ray and NMR data validated the existence of NH...O intramolecular hydrogen bonds. The formation and exchange of imines were then studied in acetonitrile, and the acidity of OH/NH significantly influenced the thermodynamics and kinetics of imine reactions. Furthermore, the role of OH/NH...N hydrogen bonds on imines was elucidated by the shift of aldehyde exchange equilibrium. Finally, the formation of imines was achieved in aqueous solutions. The mechanistic insights could pave the way for future applications in assembly and labelling.

© 2020 Elsevier Ltd. All rights reserved.

1. Introduction

Building on the reversible formation and exchange of covalent bonds, the field of dynamic covalent chemistry (DCC) has been flourishing over the past decade [1] and has found wide applications in the creation of molecular assemblies [2], identification of receptors [3], and modulation of functional materials [4]. Recently, the interplay between different dynamic covalent reactions (DCRs) and the combination of reversible covalent and supramolecular interactions are capturing significant attention, as a vessel composed of multiple dynamic bonding forces can generate structural and functional diversity and therefore build up systematic complexity [5]. As one class of the most employed reversible covalent bonds, the condensation of a carbonyl, commonly an aldehyde, and a primary amine to afford an imine (i.e. a Schiff base)

as well as associated imine exchange [6], has been integrated into many research endeavors, such as assemblies [7], catalysis [8], and sensing [9]. Therefore, there is continuous interest in developing new motifs and exploring different ways to control the imines despite their rich history.

Among the most fundamental supramolecular interactions, hydrogen bonds play a critical role in chemistry and biology, and are in the backbone of nature and synthetic materials [10]. In light of their strong directivity, tunable strength, and sensitivity to environment [10] hydrogen bonds have been frequently incorporated into dynamic assemblies [11]. Of particular interest are salicylaldehyde derivatives and their imines, which are key building blocks in organic synthesis and supramolecular chemistry [12]. The imine of salicylaldehyde is stabilized through resonance-assisted hydrogen bonding and enamine/imine tautomerism (Fig. 1a) [13]. By taking use of those effects covalent organic frameworks exhibiting enhanced stability were built, with utility in gas storage, separation, and catalysis [14]. In addition, the aforementioned hydrogen bond and tautomerism are closely associated with fluorescence signaling mechanism of excited state intramolecular proton transfer [15]. Moreover, salicylaldehyde analogs were employed for the chirality recognition of primary amines and labelling of peptides/proteins [16]. In addition, a variety of salen

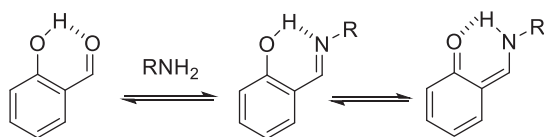
* Corresponding author. State Key Laboratory of Structural Chemistry, Fujian Institute of Research on the Structure of Matter, Chinese Academy of Sciences, Fuzhou 350002, PR China.

** Corresponding author. State Key Laboratory of Structural Chemistry, Fujian Institute of Research on the Structure of Matter, Chinese Academy of Sciences, Fuzhou 350002, PR China.

E-mail addresses: chenhang@fjirsm.ac.cn (H. Chen), lyou@fjirsm.ac.cn (L. You).

¹ These authors contributed equally to this work.

a. Previous Work :



b. This Work :

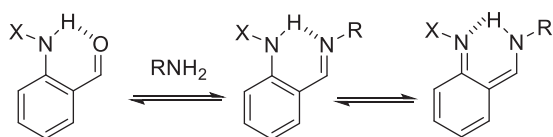


Fig. 1. The change from salicylaldehyde and its imine (a) to *ortho*-aminobenzaldehydes and associated imines (b).

complexes contributed to the development of coordination assembly and asymmetric catalysis [17].

Considering the importance of *ortho*-OH in salicylaldehyde (**1A**) [12–17], we wondered about the replacement of OH with NH (Fig. 1b). As compared to salicylaldehyde, the NH of amide/sulfonamide would also serve as a hydrogen bond donor for aldehyde/imine, but has the advantage of structural variability through facile modification of carboxylic acids/sulfonic acids. Furthermore, the tunable acidity of NH could accordingly affect its capability of forming hydrogen bonds, thereby providing a handle for ensuing DCR with primary amines. In the current work, a suit of *ortho*-

aminobenzaldehydes were prepared, and the formation and exchange of their imines were investigated in detail. The effect of hydrogen bonding on imine DCC was elucidated, and the creation of imines in aqueous solutions was further studied, providing structural and mechanistic insights for future design.

2. Results and discussions

2.1. Design and synthesis

As model compounds acetyl and methanesulfonyl derived 2-aminobenzaldehydes (**2A** and **3A**) were chosen in conjunction with their corresponding water soluble counterparts (**5A** and **6A**, Fig. 2a). Salicylaldehyde (**1A**) and its analog **4A** were employed as controls. The associated imines of aldehydes **1A–6A** were termed as **1I–6I**. The synthesis of aldehydes is shown in Fig. 2b. **2A** and **3A** were furnished by the condensation of formyl chloride/methanesulfonyl chloride with protected amine **PA**, followed by acidic hydrolysis of acetal to afford the aldehyde. In order to improve the water solubility, an acetic acid group was attached in **5A** and **6A**. Analogous acetylation, subsequent nucleophilic substitution with ethyl 2-bromoacetate, and then ester hydrolysis afforded desired **5A**. The same method to synthesis aldehyde **6A** failed, likely due to the different reactivity of NH in sulfonamide and amide. Instead, a sequence composed of the incorporation of acetic acid unit and then sulfonylation gave **6A** successfully. The aldehyde **4A** was prepared via etherification of 2,4-dihydroxybenzaldehyde. The final products were fully characterized by ¹H NMR and ¹³C NMR, as well as mass spectrometry (Figs. S1–S12).

In order to reveal the structural characteristics, especially the existence of intramolecular hydrogen bonding, single-crystal X-ray

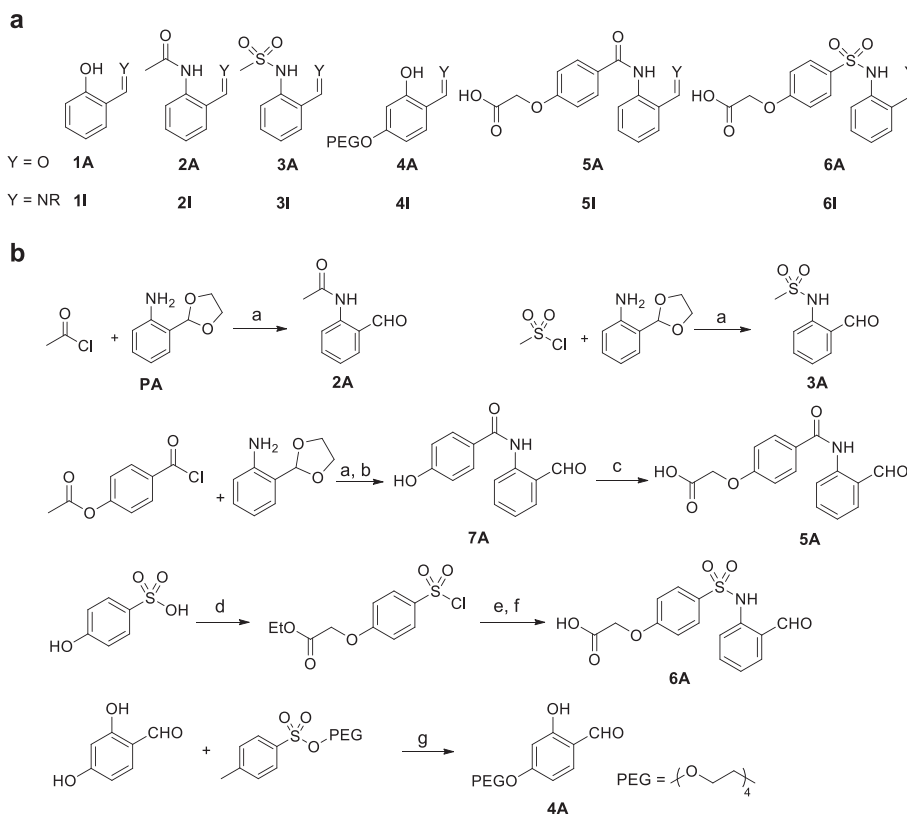


Fig. 2. (a) The design of aldehydes **1A–6A** and their imines **1I–6I**; (b) The synthesis of aldehydes. Reagents and conditions: (a) (i) pyridine, CH₂Cl₂, 0 °C; (ii) TFA, room temperature; (b) NaOH, CH₃OH, room temperature; (c) (i) ethyl bromoacetate, K₂CO₃, DMF, room temperature; (d) (i) ethyl bromoacetate, K₂CO₃, DMF; (ii) SOCl₂, refluxing; (e) (i) **PA**, pyridine, CH₂Cl₂, 0 °C; (ii) TFA, room temperature; (f) NaOH, CH₃OH, room temperature; (g) K₂CO₃, CH₃CN, refluxing.

diffraction analysis was conducted (Table S1). Taking **3A** as an example, the aldehyde and sulfonamide NH are coplanar with the benzene ring (Fig. 3). A distance of 1.97 Å was found between NH and aldehyde oxygen (NH...O), suggesting an attractive interaction. Furthermore, the NH peak of **3A** appeared at 10.5 ppm in CD₃CN (Fig. 3). Such a downfield position is also in consistence with the presence of an intramolecular hydrogen bond. For comparison, the OH or NH proton of **1A** and **2A** was found around 11.0 ppm (Table 1), again matching intramolecular hydrogen bonding. Molecular modeling also confirmed the presence of an intramolecular hydrogen bond within **1A–3A**. In all, evidences were collected to support hydrogen bonding in both solid state and solution.

2.2. Imine formation

With aldehydes in place their dynamic covalent reactions (DCRs) with primary amines were then performed in the presence of molecular sieves. Gratifyingly, the individual reactions of aldehydes **1A–3A** with 1-butylamine afforded the desired imine products (**1I–3I**) in nearly quantitative yield (Figs. S13–S15). For example, the formyl resonance of **3A** at 10.0 ppm disappeared, with the emergence of a new peak around 8.4 ppm, indicative the formation of imine. Moreover, the NH proton of **3I** resided around 12.7 ppm, significantly different from the value in **3A** (10.5 ppm,

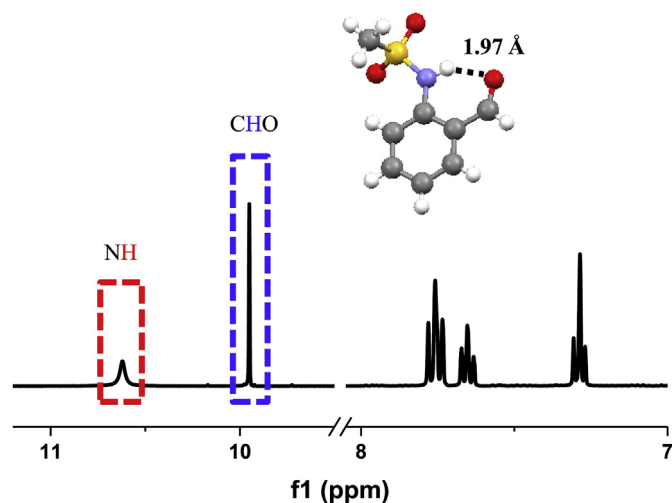


Fig. 3. ¹H NMR spectrum (CD₃CN) and X-ray structure of **3A**.

Table 1

Summary of chemical shift values (δ , in ppm) of aldehyde/imine CH and OH/NH of **1–3** in CD₃CN.

Structure	Y	Compound Number	δ (CHY)	δ (OH/NH)
	O	1A	9.93	10.94
	NBu	1I	8.44	13.65
	O	2A	9.93	10.97
	NBu	2I	8.42	12.83
	O	3A	9.94	10.50
	NBu	3I	8.44	12.74

Table 1). An analogous downfield shift of OH/NH in **1I** and **3I** was apparent in relative to **1A** and **3A**, respectively (Table 1). These findings point toward intramolecular hydrogen bonding within **1I–3I**.

The kinetics of imine formation was next followed. To gauge the reactivity the reactions were run in CD₃CN without molecular sieves (Figs. S16–S18). Aldehydes **1A** and **3A** had the same tendency, with the reaction completed in about 1 h (1.2 equiv. 1-butylamine). However, the rate of imine formation of aldehyde **2A** was much slower than that of **1A** and **3A** (Fig. 4), and it took about 30 h to equilibrate even with more 1-butylamine (2.2 equiv.). The difference in rates can be explained from the perspective of intramolecular acid catalysis: the stronger acidity of OH in **1A** and NH in **3A** results in the acceleration of imine formation, while the NH in **2A** would play a minor role due to its lower acidity, leading to the sluggish kinetics. Phenol, methanesulfonamide, acetamide have a pK_a of 18.0, 17.5, and 25.5 in DMSO, respectively [18], and the sequence of pK_a values falls in line with the trend of rates.

2.3. Imine exchange

The next goal was to check the reversibility of imine chemistry. Toward this end, component exchange of amines was investigated. Taking **3A** as an example, its reaction was first conducted with 1-butylamine, and cyclohexylamine was then added into the mixture (Fig. 5A). After the equilibrium was reached there was a decrease in the amount of imine incorporating 1-butylamine, with the concomitant appearance of cyclohexylamine derived imine (c of Fig. 5A). An equilibrium constant (*K*) of 1.90 was obtained, in favoring of the imine of 1-butylamine and also in agreement with steric effect. These findings indicate that amine exchange was occurring, thereby demonstrating the dynamic nature of the system. Moreover, the opposite sequence of amine addition (d of Fig. 5A) as well as the one-pot amine exchange (e of Fig. 5A) afforded the same equilibrium position, further validating the reversibility. Similar results on dynamic amine exchange were also obtained with **1A** (Figs. S22–S24) and **2A** (Figs. S25–S27).

To dissect the contribution of hydrogen bonding interactions on imine DCC, aldehyde exchange experiments were further performed. The equilibrium of aldehyde exchange could serve as a barometer to probe the relative affinity of aldehydes **1–3** toward amines. The stepwise aldehyde exchange was attempted, as

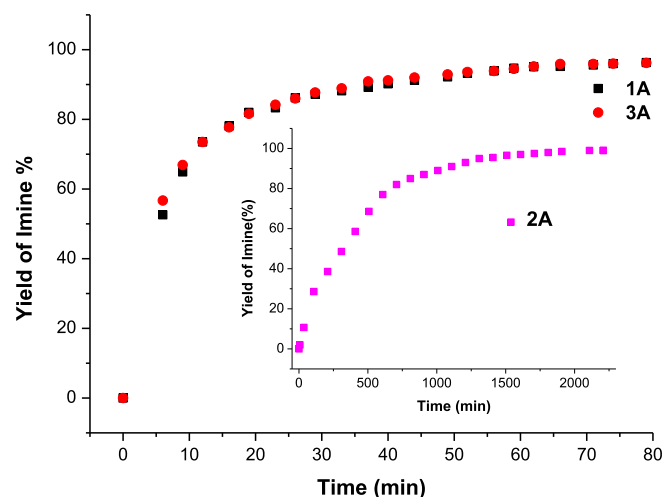


Fig. 4. Kinetic profile of the creation of imines **1I–3I** from individual reactions of **1A–3A** (15 mM) and 1-butylamine (1.2 equiv. for **1A** and **3A**; 2.2 equiv. for **2A**) at 25 °C.

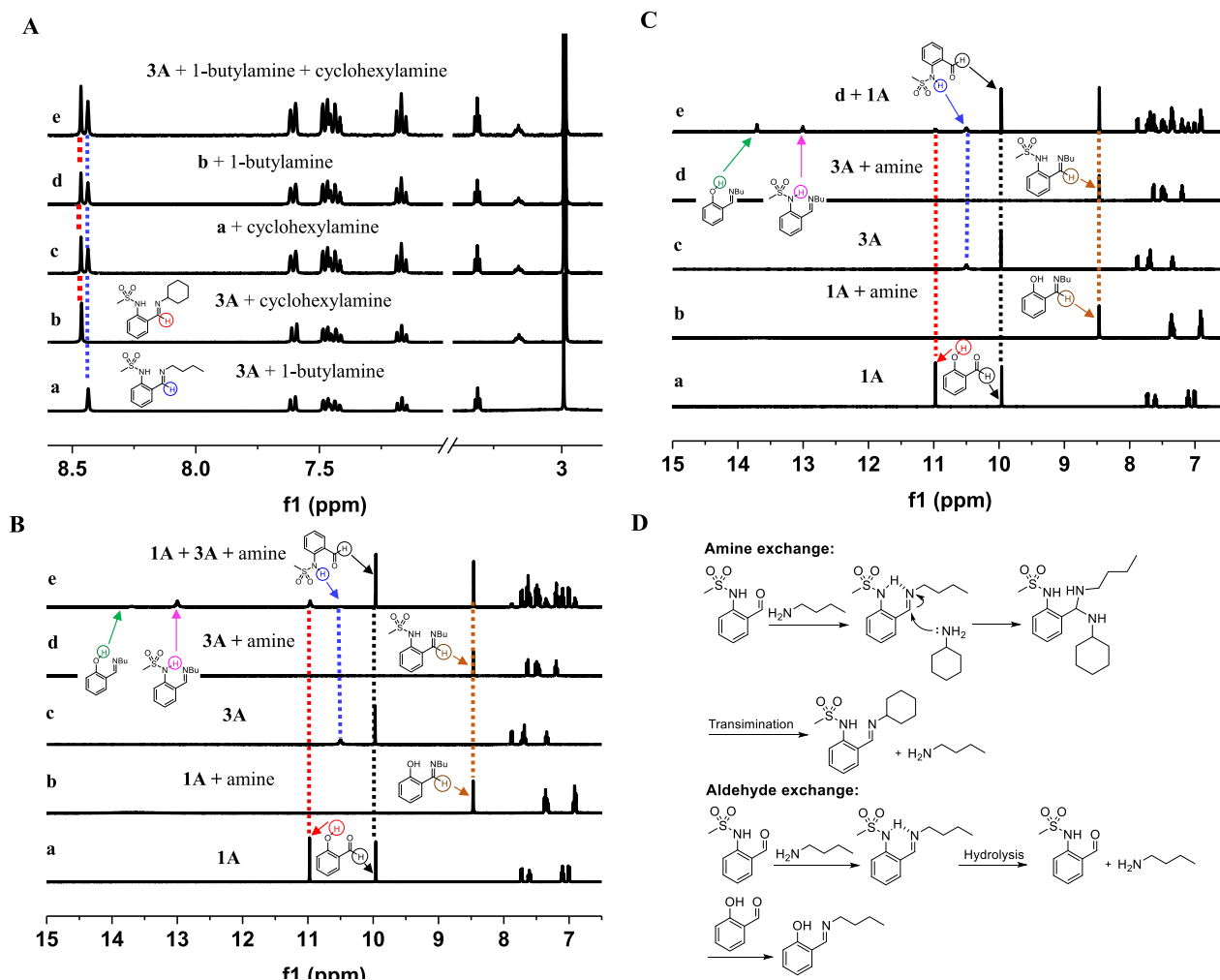


Fig. 5. (A) Amine exchange: (a) the reaction of **3A** with 1-butylamine (1.2 equiv.); (b) the reaction of **3A** with cyclohexylamine (1.2 equiv.); (c) the addition of cyclohexylamine (1.2 equiv.) into (a); (d) the addition of 1-butylamine (1.2 equiv.) into (b); (e) the reaction of **3A** with 1-butylamine (1.2 equiv.) and cyclohexylamine (1.2 equiv.). (B) Sequential aldehyde exchange: (a) **1A**; (b) the reaction of **1A** with 1-butylamine (1.0 equiv.); (c) **3A**; (d) the reaction of **3A** with 1-butylamine (1.0 equiv.); (e) the addition of **1A** (1.0 equiv.) into (d). (C) One-pot aldehyde exchange: (a) **1A**; (b) the reaction of **1A** with 1-butylamine (1.0 equiv.); (c) **3A**; (d) the reaction of **3A** with 1-butylamine (1.0 equiv.); (e) the reaction of **1A**, **3A** (1.0 equiv.), and 1-butylamine (1.0 equiv.). (D) Proposed mechanism of sequential amine exchange and aldehyde exchange. Solvent: CD_3CN .

forementioned amine exchange. For example, **1A** was added into preformed **3I** (Fig. 5B). The aldehyde exchange was notoriously slow, and only a small amount of **1I** were apparent in ^1H NMR spectra even after one year (e of Fig. 5B and Fig. S38). Similar slow sequential aldehyde exchange was found with other aldehyde combinations (Figs. S31–S34). These observations were rationalized with the stabilizing effect of intramolecular hydrogen bonding on imine, which renders hydrolysis of imine difficult. The decomposition of imine to recover the original aldehyde and amine could be required for its reaction with the second aldehyde to complete the sequential aldehyde exchange. In contrast, amine exchange could proceed via a transimination pathway, circumventing the hydrolysis of imine (Fig. 5D).

The competition between salicylaldehyde (**1A**) and aldehyde **2A/3A** for the reaction with 1-butylamine was therefore run in one-pot. The equilibrium was readily reached in three days. For example, with both **1A** and **3A** present in the reaction mixture, their imines were detected (Figs. 5C and S40). A K value of 1.84 was revealed, preferring the imine of salicylaldehyde (**1I**) and **3A**. Imine **1I** was dominant for the reaction of **1A**, **2A**, and 1-butylamine, as

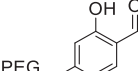
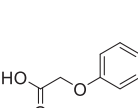
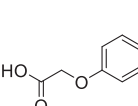
reflected by a K value of 345 and in favor of **1I** (Fig. S39). The competition between **2A** and **3A** for the reaction with 1-butylamine also strongly favored the imine of **3A** (K around 170) (Fig. S41). These results suggest that **1A** and **3A** show comparable affinity for primary amines, while aldehyde **2A** is much worse than **1A** and **3A**. The trend approximately echoes the sequence of OH/NH acidity and reinforces the critical role of hydrogen bonding on the thermodynamic stability of imines.

Inspired by significantly different outcomes between sequential and one-pot aldehyde exchanges, the lability of imines in aqueous media was explored. Water was added into preformed imine products in acetonitrile to give a solvent mixture (3:1 $\text{CD}_3\text{CN}/\text{D}_2\text{O}$), and NMR spectra were tracked to gain a deeper understanding of the stability of imines toward the hydrolysis and regeneration of the initial reactants (Figs. S42–S44). After 7 days very little decomposition of imine was found (less than 5%). We thereby inferred that hydrogen bond can modulate the stability of imine in mixed solvents, although the use of water facilitates the reverse reaction, albeit to a small degree.

2.4. Imine formation in aqueous solutions

Finally, the formation and exchange of imines were explored in purely aqueous media. In recent years studies on supramolecular chemistry in water, the working environment of nature, are generating intensive interest [19]. Reactions of **4A**, **5A**, and **6A** and 1-butylamine in water (Figs. S45–S48) gave imines **4I**, **5I**, and **6I** with a yield of 63%, 35%, and 42%, respectively (Fig. 6a and Table 2). Interestingly, the equilibrium was rapidly reached after 5 min for **5A** and **6A**, while it took 50 min for the reaction of **4A** to equilibrate (Fig. 6a). One rationalization comes from partial deprotonation of OH in **4A** in basic aqueous media, compromising intramolecular acid catalysis. On the other hand, the stronger acidity of NH of **5A** and **6A** in water than in acetonitrile could contribute to their relatively fast kinetics. The competition between **4A** and **6A** for the reaction with 1-butylamine was feasible, giving a *K* value of 3.70 and favoring **4I** (Figs. 6b and S51). Such a finding is in agreement with the trend of yield for imine formation reactions.

Table 2
Summary of the yield of imine formation in aqueous media.

Aldehyde	Structure	D ₂ O	pH 7.0 Buffer	pH 7.4 Buffer	pH 8.0 Buffer
4A		63%	39%	45%	52%
5A		35%	NR ^a	NR	NR
6A		42%	20%	22%	26%

^a NR stands for no reaction.

The buffer solutions (50 mM, PBS buffer) of **4A**, **5A**, and **6A** at different pH were then prepared, and their reactions with 1-butylamine were monitored. Aldehydes **4** and **6** afforded their corresponding 1-butylamine derived imines with a yield of 45% and 21% at pH 7.4, respectively (Table 2 and Figs. S52 and S56). However, no imine of **5** was detected under similar condition (Fig. S55). These results are reminiscent of the trend of aldehyde exchange in acetonitrile, as the acidity and hydrogen bonding ability of OH/NH have a pronounced impact on the reactivity and stability of imine DCC. As the pH increased, there was an enhancement in the yield of the imine (Table 2). As the case of reactions in water, the imine formation in buffer proceeded more quickly for **6A** than **4A** (Figs. S53 and S57). Therefore, both thermodynamics and kinetics of imine chemistry can be tuned in aqueous solutions.

3. Conclusions

In summary, a suite of salicylaldehyde analogs were prepared, and their associated imine chemistry was explored in detail. The presence of intramolecular NH...O hydrogen bond was supported by X-ray and NMR data. The formation of imines was then studied in acetonitrile, and the acidity of OH/NH was found to significantly impact the thermodynamics and kinetics of imine reactions. Moreover, the reversibility of system was verified by amine exchange, and the extent of aldehyde exchange equilibrium provided insights for the modulation of imine through intramolecular hydrogen bonding. Finally, the formation and exchange of imines were realized in aqueous media, showing application potential in biolabelling. The current platform complements salicylaldehyde and its imines and further demonstrates the ability of neighboring supramolecular interactions for dictating imine chemistry.

4. Experimental section

4.1. General

¹H NMR and ¹³C NMR spectra were recorded on a 400 MHz Bruker Biospin Avance III spectrometer. The chemical shifts (δ) for ¹H NMR spectra, given in ppm, are referenced to the residual proton signal of the deuterated solvent. Mass spectra were recorded on a Bruker IMPACT-II spectrometer. The pH value was measured on a Sartorius PB-10 pH meter. All reagents were obtained from commercial sources and were used without further purification, unless indicated otherwise.

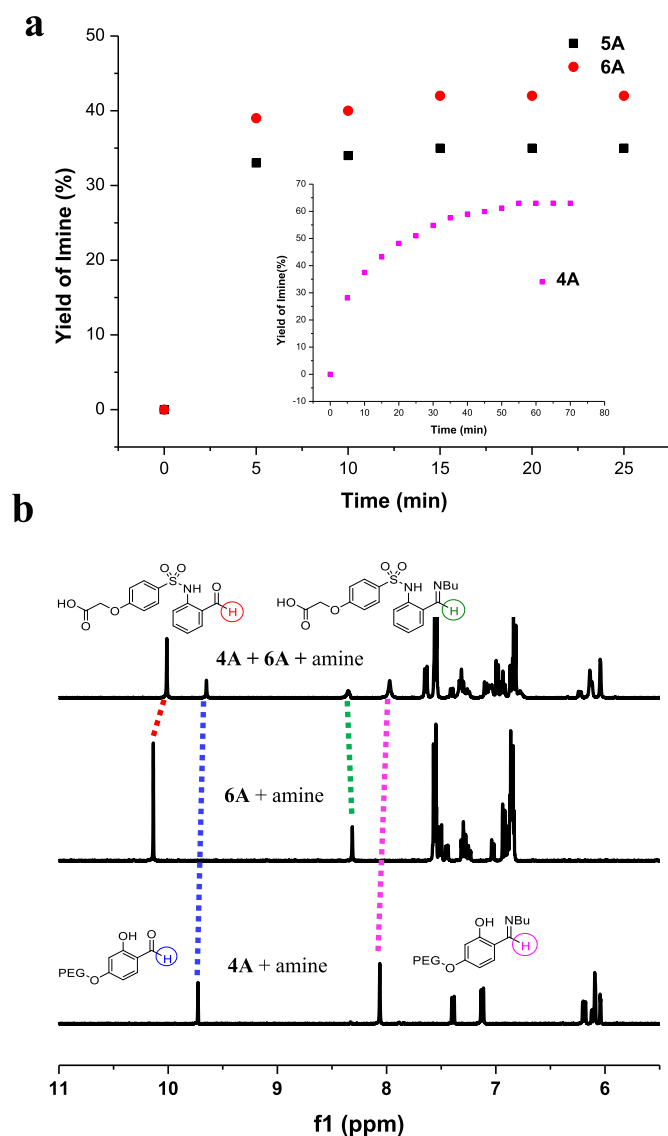


Fig. 6. (a) Kinetic profile of the creation of imines **4I–6I** from individual reactions of **4A–6A** (15 mM) and 1-butylamine (2.2 equiv. for **5A** and **6A**; 1.2 equiv. for **4A**) in D₂O at 25 °C; (b) The competition between **4A** (1.0 equiv.) and **6A** (1.0 equiv.) for the reaction with 1-butylamine (2.0 equiv.) in D₂O.

4.2. DCRs in acetonitrile

Dynamic covalent reactions (DCRs) were performed *in situ* in the presence of molecular sieves (3 Å) in CD₃CN at room temperature (25 °C) without isolation and purification. For imine formation reactions, to an aldehyde (~15 mM, 1.0 equiv.) in CD₃CN (0.60 mL), was added an amine (RNH₂, 1.2 equiv.). For aldehyde exchange reactions two aldehydes (~15 mM each, 1.0 equiv.) were mixed with 1-butylamine (1.0 equiv.) in CD₃CN. For amine exchange reactions, the aldehyde (~15 mM each, 1.0 equiv.) was first mixed with one primary amine (1.2 equiv.) in CD₃CN (0.60 mL), and after equilibration the second amine (1.2 equiv.) was added. The mixture was stirred and then characterized by ¹H NMR and ESI-MS after the equilibrium was reached. Integrals from ¹H NMR spectra (aldehydes and imines) were used for the calculation of equilibrium constants. See figure captions for specific conditions if necessary.

4.3. DCRs in aqueous solution

For imine formation in water, the aldehyde (~15 mM) and 1-butylamine were dissolved in D₂O (0.60 mL). For aldehyde exchange reaction two aldehydes (~15 mM each, 1.0 equiv.) were mixed with 1-butylamine (2.0 equiv.) in D₂O. For imine formation in 50 mM phosphate buffer (PB) in D₂O, the stock solutions of aldehydes **4A**, **5A**, and **6A** (15 mM) were prepared in PB buffer, respectively, and the desired pH (7.0, 7.4, or 8.0) was adjusted with concentrated NaOH or HCl solution. To an aldehyde (15 mM, 1.0 equiv.) solution in PB buffer, was added 1-butylamine (1.2 equiv.). The mixture was equilibrated at room temperature (25 °C) and characterized by ¹H NMR and ESI-MS. See figure captions for specific conditions if necessary.

4.4. Synthesis

The synthetic route and structures of the target compounds are shown in Fig. 2.

4.4.1. 2-(1,3-dioxolan-2-yl)aniline (PA)

The reported procedure [20] was used to afford the title compound as a yellow oil.

4.4.2. N-(2-formylphenyl)acetamide (2A)

A solution of the **PA** (0.50 g, 1.0 equiv.) and pyridine (0.30 mL, 1.2 equiv.) in dry dichloromethane (DCM, 30 mL) was cooled in an ice bath, and a solution of acetyl chloride (0.35 mL, 1.5 equiv.) in DCM (5.0 mL) was added dropwise. Upon completion after 1 h, the solution was washed with dilute trifluoroacetic acid, and the mixture was extracted with ethyl acetate. The combined organic layer was washed with saturated NaHCO₃, dried with anhydrous Na₂SO₄, and concentrated *in vacuo*. The residue was then purified by column chromatography (silica gel, petroleum ether (PE)/ethyl acetate (EA) = 4:1) to afford the title compound as a white solid (0.40 g, 81%). ¹H NMR (CDCl₃): δ 11.13 (s, 1 H), 9.92 (s, 1 H), 8.76 (d, J = 8.4 Hz, 1 H), 7.70 (dd, J = 7.6, 1.2 Hz, 1 H), 7.64 (td, J = 7.2, 1.6 Hz, 1 H), 7.25 (td, J = 6.6, 1.2 Hz, 1 H), 2.26 (s, 3 H). ¹³C NMR (CDCl₃) δ 195.6, 169.7, 140.9, 136.3, 136.1, 122.9, 121.5, 119.8, 25.4. ESI-HRMS: *m/z* calcd for C₉H₉NO₂Na [M + Na⁺]: 186.0531; found: 186.0532.

4.4.3. N-(2-formylphenyl)methanesulfonamide (3A)

A solution of the **PA** (0.50 g, 1.0 equiv.) and pyridine (0.30 mL, 1.2 equiv.) in dry dichloromethane (DCM, 30 mL) was cooled in an ice bath, and a solution of acetyl chloride (0.45 mL, 1.5 equiv.) in DCM (5.0 mL) was added dropwise. Upon completion after 1 h, the solution was washed with dilute trifluoroacetic acid, and the mixture was extracted with ethyl acetate. The combined organic layer was

washed with saturated NaHCO₃, dried with anhydrous Na₂SO₄, and concentrated *in vacuo*. The residue was then purified by column chromatography (silica gel, PE/EA = 4:1) to afford the title compound as a white solid (0.48 g, 80%). ¹H NMR (CDCl₃): δ 10.60 (s, 1 H), 9.92 (s, 1 H), 7.76 (t, J = 7.6, 1.2 Hz, 2 H), 7.65 (t, J = 6.6 Hz, 1 H), 7.28 (dd, J = 10.9, 4.2 Hz, 1 H), 3.13 (s, 3 H). ¹³C NMR (CDCl₃) δ 195.2, 140.3, 136.6, 136.3, 123.1, 121.7, 117.0, 40.4. ESI-HRMS: *m/z* calcd for C₈H₉NO₃Na [M + Na⁺]: 222.0201; found: 222.0201.

4.4.4. 4-((2,5,8,11-tetraoxatridecan-13-yl)oxy)-2-hydroxybenzaldehyde (4A)

To a suspension of 2,5,8,11-tetraoxatridecan-13-yl 4-methylbenzenesulfonate (0.40 g, 1.0 equiv.) and potassium carbonate (0.31 g, 2.0 equiv.) in anhydrous CH₃CN (10.0 mL), was added 2,4-dihydroxybenzaldehyde (0.19 g, 1.2 equiv.) under N₂ atmosphere. The reaction was refluxed overnight. After the reaction was cooled to room temperature, the solution was washed with dilute hydrochloric acid and extracted with ethyl acetate. The combined organic layer was washed with saturated NaHCO₃, and brine solution and then dried with anhydrous Na₂SO₄. After the removal of solvent under vacuum and further purification by column chromatography (silica gel, PE/EA = 1:1), the title compound was obtained as a brown oil (0.20 g, 55%). ¹H NMR (D₂O): δ 9.56 (s, 1H), 7.49 (d, J = 5.6 Hz, 1H), 6.52 (dd, J = 6.8, 1.2 Hz, 1H), 6.36 (d, J = 2.4 Hz, 1H), 4.12 (t, J = 4.0 Hz, 2H), 3.77 (t, J = 4.0 Hz, 2H), 3.63–3.61 (m, 2H), 3.57–3.49 (m, 8H), 3.45–3.42 (m, 2H), 3.2 (s, 3H). ¹³C NMR (D₂O): δ 195.9, 165.7, 162.5, 136.0, 115.4, 108.5, 101.3, 71.6, 70.9, 69.7, 69.5, 69.4, 69.3, 68.7, 67.4, 57.9. ESI-HRMS: *m/z* calcd for C₁₆H₂₄O₇Na [M + Na⁺]: 351.1420; found: 351.1421.

4.4.5. N-(2-formylphenyl)-4-hydroxybenzamide (7A)

A solution of the **PA** (0.50 g, 1.0 equiv.) and pyridine (0.30 mL, 1.2 equiv.) in dry dichloromethane (DCM, 30 mL) was cooled in an ice bath, and a solution of 4-(chlorocarbonyl)phenyl acetate (0.90 g, 1.5 equiv.) in DCM (5.0 mL) was added dropwise. Upon completion after 2 h, the solution was washed with dilute trifluoroacetic acid, and the mixture was extracted with ethyl acetate. The combined organic layer was then washed with saturated NaHCO₃, dried with anhydrous Na₂SO₄, and concentrated *in vacuo*. The crude product was dissolved in methanol (5.0 mL), and 2 M NaOH (5.0 mL) was added for the hydrolysis of the ester. After stirring overnight the mixture was extracted with ethyl acetate, and the combined organic layer was washed with brine solution, dried with anhydrous Na₂SO₄, and concentrated *in vacuo*. The residue was then purified by column chromatography (silica gel, PE/EA = 3:1) to afford the title compound as a white solid (0.35 g, 48%). ¹H NMR (DMSO-*d*₆): δ 11.68 (s, 1H), 10.35 (s, 1H), 10.04 (s, 1H), 8.55 (d, J = 8.0 Hz, 1H), 7.96 (dd, J = 7.6, 1.6 Hz, 1H), 7.86 (d, J = 8.0 Hz, 2H), 7.73 (td, J = 7.6, 1.6 Hz, 1H), 7.35 (t, J = 7.2 Hz, 1H), 6.95 (d, J = 8.0 Hz, 2H). ¹³C NMR (DMSO-*d*₆): δ 196.7, 165.6, 161.9, 141.0, 136.4, 135.8, 129.9, 124.9, 123.9, 123.7, 120.5, 116.1. ESI-HRMS: *m/z* calcd for C₁₄H₁₁NO₃Na [M + Na⁺]: 264.0637; found: 264.0638.

4.4.6. 2-(4-((2-formylphenyl)carbamoyl)phenoxy)acetic acid (5A)

To a suspension of N-(2-formylphenyl)-4-hydroxybenzamide (0.50 g, 1.0 equiv.) and potassium carbonate (0.43 g, 1.5 equiv.) in anhydrous DMF (10.0 mL), a solution of ethyl bromoacetate (0.42 g, 1.2 equiv.) in DMF (3.0 mL) was added dropwise. The reaction was stirred at room temperature overnight. Afterwards H₂O was added, and the mixture was extracted with ethyl acetate. The combined organic layer was washed with brine, dried over anhydrous Na₂SO₄, and concentrated *in vacuo*. The crude product was dissolved in methanol (5.0 mL), and 2 M NaOH (5.0 mL) was added for the hydrolysis of the ester. After stirring overnight the mixture was extracted with ethyl acetate, and then the combined organic layer

was washed with brine solution, dried with anhydrous Na_2SO_4 , and concentrated *in vacuo*. The residue was then purified by column chromatography (silica gel, PE/EA = 1:1) to afford the title compound as a white solid (0.39 g, 63%). ^1H NMR ($\text{DMSO}-d_6$): δ 11.69 (s, 1H), 10.06 (s, 1H), 8.53 (d, J = 8.0 Hz, 1H), 7.99–7.96 (m, 3H), 7.76 (td, J = 8.0, 1.2 Hz, 1H), 7.38 (td, J = 7.6, 1.6 Hz, 1H), 7.15 (d, J = 8.0 Hz, 2H), 4.84 (s, 2H). ^{13}C NMR ($\text{DMSO}-d_6$): δ 196.5, 170.3, 165.4, 161.5, 140.8, 136.3, 135.6, 129.7, 127.0, 124.2, 123.9, 120.7, 115.3, 65.1. ESI-HRMS: m/z calcd for $\text{C}_{16}\text{H}_{13}\text{NO}_5\text{Na}$ [$\text{M} + \text{Na}^+$]: 322.0691; found: 322.0691.

4.4.7. Ethyl 2-(4-(chlorosulfonyl)phenoxy)acetate

The reported procedure [21] was used to afford the title compound as a colorless viscous liquid.

4.4.8. 2-(4-(N-(2-formylphenyl)sulfamoyl)phenoxy)acetic acid (6A)

A solution of the **PA** (0.50 g, 1.0 equiv.) and pyridine (0.30 mL, 1.2 equiv.) in dry dichloromethane (DCM, 30 mL) was cooled in an ice bath, and a solution of ethyl 2-(4-(chlorosulfonyl)phenoxy)acetate (1.27 g, 1.5 equiv.) in DCM (5.0 mL) was added dropwise. Upon completion after 2 h, the solution was washed with dilute trifluoroacetic acid, and the mixture was extracted with ethyl acetate. The combined organic layer was then washed with saturated NaHCO_3 , dried with anhydrous Na_2SO_4 , and concentrated *in vacuo*. The crude product was dissolved in methanol (5.0 mL), and 2 M NaOH (5.0 mL) was added for the hydrolysis of the ester. After stirring overnight the mixture was extracted with ethyl acetate, and the combined organic layer was washed with brine solution, dried with anhydrous Na_2SO_4 , and concentrated *in vacuo*. The residue was then purified by column chromatography (silica gel, PE/EA = 1:1) to afford the title compound as a yellow solid (0.20 g, 20%). ^1H NMR ($\text{DMSO}-d_6$): δ 10.54 (s, 1H), 10.02 (s, 1H), 7.82 (dd, J = 6.0, 1.6 Hz, 1H), 7.66 (d, J = 8.0 Hz, 2H), 7.59 (td, J = 8.0, 1.2 Hz, 1H), 7.33 (t, J = 8.0 Hz, 1H), 7.19 (d, J = 8.0 Hz, 1H), 7.05 (d, J = 8.0 Hz, 2H), 4.78 (s, 2H). ^{13}C NMR ($\text{DMSO}-d_6$): δ 193.6, 170.1, 161.9, 139.4, 135.9, 132.4, 131.1, 129.6, 127.6, 127.5, 125.8, 122.7, 115.7, 65.2. ESI-HRMS: m/z calcd for $\text{C}_{15}\text{H}_{13}\text{NO}_6\text{SNa}$ [$\text{M} + \text{Na}^+$]: 358.0361; found: 358.0361.

Declaration of competing interest

The authors declare that they have no known competing financial interests or personal relationships that could have appeared to influence the work reported in this paper.

Acknowledgement

We thank National Natural Science Foundation of China (21672214), the Recruitment Program of Global Youth Experts, and the Strategic Priority Research Program (XDB20000000) and the Key Research Program of Frontier Sciences (QYZDB-SSW-SLH030) of the Chinese Academy of Sciences for funding.

Appendix A. Supplementary data

Supplementary data to this article can be found online at <https://doi.org/10.1016/j.tet.2020.131128>.

References

- [1] (a) S.J. Rowan, S.J. Cantrill, G.R.L. Cousins, J.K.M. Sanders, J.F. Stoddart, *Angew. Chem. Int. Ed.* 41 (2002) 898–952; (b) J.-M. Lehn, *Chem. Soc. Rev.* 36 (2007) 151–160; (c) Y. Jin, C. Yu, R.J. Denman, W. Zhang, *Chem. Soc. Rev.* 42 (2013) 6634–6654; (d) Q. Ji, R.C. Lirag, O.S. Miljanić, *Chem. Soc. Rev.* 43 (2014) 1873–1884;
- (e) A. Herrmann, *Chem. Soc. Rev.* 43 (2014) 1899–1933.
- [2] (a) J.F. Reuther, J.L. Dees, I.V. Kolesnichenko, E.T. Hernandez, D.V. Ukrantsev, R. Guduru, M. Whiteley, E.V. Anslyn, *Nat. Chem.* 10 (2018) 45–50; (b) G. Zhang, M. Mastalerz, *Chem. Soc. Rev.* 43 (2014) 1934–1947; (c) Y. Jin, Y. Hu, W. Zhang, *Nat. Rev. Chem.* 1 (2017), 0056; (d) X. Feng, X. Ding, D. Jiang, *Chem. Soc. Rev.* 41 (2012) 6010–6022; (e) S.-Y. Ding, W. Wang, *Chem. Soc. Rev.* 42 (2013) 548–568; (f) S.P. Black, J.K.M. Sanders, A.R. Stefankiewicz, *Chem. Soc. Rev.* 43 (2014) 1861–1872; (g) T. Hasell, A.I. Cooper, *Nat. Rev. Mater.* 1 (2016) 16053; (h) C. Qian, Q.-Y. Qi, G.-F. Jiang, F.-Z. Cui, Y. Tian, X. Zhao, *J. Am. Chem. Soc.* 139 (2017) 6736–6743.
- [3] (a) M. Mondal, A.K. Hirsch, *Chem. Soc. Rev.* 44 (2015) 2455–2488; (b) R. Caraballo, H. Dong, J.P. Ribeiro, J. Jiménez-Barbero, O. Ramström, *Angew. Chem. Int. Ed.* 49 (2010) 589–593; (c) R.M. Miller, V.O. Paavilainen, S. Krishnan, I.M. Serafimova, J. Taunton, *J. Am. Chem. Soc.* 135 (2013) 5298–5301; (d) O. Shyshov, R.-C. Brachvogel, T. Bachmann, R. Srikantharajah, D. Segets, F. Hampel, R. Puchta, M. von Delius, *Angew. Chem. Int. Ed.* 56 (2017) 776–781.
- [4] (a) E. Moulin, G. Cormos, N. Giuseppone, *Chem. Soc. Rev.* 41 (2012) 1031–1049; (b) R. Deng, M.J. Derry, C.J. Mable, Y. Ning, S.P. Armes, *J. Am. Chem. Soc.* 139 (2017) 7616–7623; (c) F. della Sala, E.R. Kay, *Angew. Chem. Int. Ed.* 54 (2015) 4187–4191; (d) W. Edwards, N. Marro, G. Turner, E.R. Kay, *Chem. Sci.* 9 (2018) 125–133.
- [5] (a) A. Wilson, G. Gasparini, S. Matile, *Chem. Soc. Rev.* 43 (2014) 1948–1962; (b) J. Li, P. Nowak, S. Otto, *J. Am. Chem. Soc.* 135 (2013) 9222–9239; (c) D.A. Roberts, B.S. Pilgrim, J.R. Nitschke, *Chem. Soc. Rev.* 47 (2018) 626–644; (d) J.F. Reuther, S.D. Dahlhauser, E.V. Anslyn, *Angew. Chem. Int. Ed.* 58 (2019) 74–85.
- [6] (a) M.E. Belowich, J.F. Stoddart, *Chem. Soc. Rev.* 41 (2012) 2003–2024; (b) M. Ciaccia, S. Di Stefano, *Org. Biomol. Chem.* 13 (2015) 646–654.
- [7] (a) Y. Jia, J. Li, *Chem. Rev.* 115 (2015) 1597–1621; (b) Y. Liu, Z.-T. Li, *Aust. J. Chem.* 66 (2013) 9–22.
- [8] (a) P.G. Cozzi, *Chem. Soc. Rev.* 33 (2004) 410–421; (b) A. Dirksen, S. Dirksen, T.M. Hackeng, P.E. Dawson, *J. Am. Chem. Soc.* 128 (2006) 15602–15603; (c) F. Schaufelberger, O. Ramström, *J. Am. Chem. Soc.* 138 (2016) 7836–7839.
- [9] (a) X. Su, I. Arahamian, *Chem. Soc. Rev.* 43 (2014) 1963–1981; (b) H. Zou, Y. Hai, H. Ye, L. You, *J. Am. Chem. Soc.* 141 (2019) 16344–16353.
- [10] (a) P.A. Kollman, L.C. Allen, *Chem. Rev.* 72 (1972) 283–303; (b) G.K. Such, A.P.R. Johnston, F. Caruso, *Chem. Rev.* 40 (2011) 19–29; (c) M. Juanes, R.T. Saragi, W. Caminati, A. Lesarri, *Chem. Eur. J.* 25 (2019) 11402–11411; (d) J.N.N. Eildal, G. Hultqvist, T. Balle, N. Stühr-Hansen, S. Padrah, S. Gianni, K. Strømgaard, P. Jemth, *J. Am. Chem. Soc.* 135 (2013) 12998–13007; (e) R. Bu, Y. Xiong, X. Wei, H. Li, C. Zhang, *Cryst. Growth Des.* 19 (2019) 5981–5997.
- [11] (a) S. Kitagawa, K. Uemura, *Chem. Soc. Rev.* 34 (2005) 109–119; (b) J.-F. Xu, Y.-Z. Chen, D. Wu, L.-Z. Wu, C.-H. Tung, Q.-Z. Yang, *Angew. Chem. Int. Ed.* 52 (2013) 9738–9742; (c) X. Lou, R.P.M. Lafleur, C.M.A. Leenders, S.M.C. Schoenmakers, N.M. Matsumoto, M.B. Baker, J.L.J. van Dongen, A.R.A. Palmans, E.W. Meijer, *Nat. Commun.* 8 (2017) 15420.
- [12] (a) K. Maher, *Inter. Multi. Res. Rev.* 7 (2015); (b) K. Li, Y. Xiang, X. Wang, J. Li, R. Hu, A. Tong, B.Z. Tang, *J. Am. Chem. Soc.* 136 (2014) 1643–1649; (c) F. Esteban, W. Cieřlik, E.M. Arpa, A. Guerrero-Corella, S. Díaz-Tendero, J. Perles, J.A. Fernández-Salas, A. Fraile, J. Alemán, *ACS Catal.* 8 (2018) 1884–1890.
- [13] (a) C.M. Metzler, A. Cahill, D.E. Metzler, *J. Am. Chem. Soc.* 102 (1980) 6075–6082; (b) J. Crueiras, A. Rios, E. Riveiros, J.P. Richard, *J. Am. Chem. Soc.* 131 (2009) 15815–15824; (c) A.E. Felten, G. Zhu, Z.D. Aron, *Org. Lett.* 12 (2010) 1916–1919.
- [14] (a) S. Kandambeth, A. Mallick, B. Lukose, M.V. Mane, T. Heine, R. Banerjee, *J. Am. Chem. Soc.* 134 (2012) 19524–19527; (b) X. Han, Q. Xia, J. Huang, Y. Liu, C. Tan, Y. Cui, *J. Am. Chem. Soc.* 139 (2017) 8693–8697; (c) S. Yan, X. Guan, H. Li, D. Li, M. Xue, Y. Yan, V. Valtchev, S. Qiu, Q. Fang, *J. Am. Chem. Soc.* 141 (2019) 2920–2924; (d) M. Zhang, L. Li, Q. Lin, M. Tang, Y. Wu, C. Ke, *J. Am. Chem. Soc.* 141 (2019) 5154–5158.
- [15] (a) H. Houjou, H. Shingai, K. Yagi, I. Yoshikawa, K. Araki, *J. Org. Chem.* 78 (2013) 9021–9031; (b) A.C. Sedgwick, L. Wu, H.-H. Han, S.D. Bull, X.-P. He, T.D. James, J.L. Sessler, B.Z. Tang, H. Tian, J. Yoon, *Chem. Soc. Rev.* 47 (2018) 8842–8880; (c) H. Xi, Z. Zhang, W. Zhang, M. Li, C. Lian, Q. Luo, H. Tian, W.-H. Zhu, *J. Am. Chem. Soc.* 141 (2019) 18467–18474.
- [16] (a) J.M. Gilmore, R.A. Scheck, A.P. Esser-Kahn, N.S. Joshi, M.B. Francis, *Angew. Chem. Int. Ed.* 45 (2006) 5307–5311; (b) S.L. Pilicer, P.R. Bakhshi, K.W. Bentley, C. Wolf, *J. Am. Chem. Soc.* 139 (2017) 1758–1761;

- (c) D.P. Murale, S.C. Hong, S.-y. Jang, J.-S. Lee, *Chembiochem* 19 (2018) 2545–2549.
- [17] (a) S. Shaw, J.D. White, *Chem. Rev.* 119 (2019) 9381–9426;
(b) J.C. Pessoa, I. Correia, *Coord. Chem. Rev.* 388 (2019) 227–247.
- [18] F.G. Bordwell, *Acc. Chem. Res.* 21 (1988) 456–463.
- [19] (a) S. Ulrich, *Acc. Chem. Res.* 52 (2019) 510–519;
(b) M.J. Langton, C.J. Serpell, P.D. Beer, *Angew. Chem. Int. Ed.* 55 (2016) 1974–1987.
- [20] Z.A. De los Santos, C. Wolf, *J. Am. Chem. Soc.* 138 (2016) 13517–13520.
- [21] Y. Li, Z. Li, F. Li, Q. Wang, F. Tao, *Org. Biomol. Chem.* 3 (2005) 2513–2518.